INT. J. REMOTE SENSING, 2001, VOL. 22, NO. 17, 3503–3520

Sensitivity of vegetation indices to substrate brightness in hyper-arid environment: the Makhtesh Ramon Crater (Israel) case study

H. SCHMIDT and A. KARNIELI†

Remote Sensing Laboratory, J. Blaustein Institute for Desert Research, Ben-Gurion University of the Negev, Sede Boker Campus 84990, Israel

(*Received 13 November 1998; in final form 25 May 2000*)

Abstract. The influence of soil background on most vegetation indices (VIs) derived from remotely sensed imagery is a well known phenomenon, and has generated interest in the development of indices that would be less sensitive to this influence. Several such indices have been developed thus far. This paper focuses on testing and comparing the sensitivity of seven intensively used, Landsat Thematic Mapper (TM) derived, VIs (NDVI, SAVI, MSAVI, PVI, WDVI, $SAVI_2$ and TSAVI) to bare surface variation with almost no vegetation signal. The study was conducted on a terrain composed of a high variety of bare surface materials of which basalt and gypsum are two extremely dark and bright substrates respectively. It was found that SAVI and MSAVI respond to bare surface material very similarly. Such close similarity was also found between PVI and WDVI, and between $SAVI_2$ and TSAVI. NDVI tends to be overestimated on dark surfaces, while SAVI, PVI and TSAVI show more sensitivity to bright surfaces. Comparison between Δ_{VI} (the difference between pairs of VIs) and the brightness of the different surface materials showed a high correlation in each case, which underlines the fact that the response of different VIs to bare surface variation is mainly related to the surface brightness.

1. Introduction

Different vegetation indices (VIs), based on combinations of two or more spectral bands, have been developed over the last three decades because more information about the state of vegetation and its characteristics (spatial coverage, biomass, productivity, etc.) can be derived more accurately from multi-band analysis than from a single band. Most VIs are computed from radiance, reflectance, or at least apparent reflectance values in the red and the near-infrared (NIR) bands (Bannari *et al.* 1995)

The most commonly applied vegetation index for agricultural and ecological applications is the Normalized Difference Vegetation Index (NDVI, table 1), which has been shown to be widely usable for vegetation analysis (Rouse *et al.* 1974). Previous studies have shown that multi-temporal NDVI images are useful for analys-

†e-mail: Karnieli@bgumail.bgu.ac.il

International Journal of Remote Sensing
ISSN 0143-1161 print/ISSN 1366-5901 online
http://www.tandf.co.uk/journals
DOI: 10.1080/01431160110063779

Table 1. Vegetation indices used in this study.

Vegetation index	Reference
Normalized Difference Vegetation Index $NDVI = \frac{(NIR - R)}{(NIR + R)}$	Rouse *et al.* (1974)
Perpendicular Vegetation Index $PVI = \frac{(NIR - aR - b)}{\sqrt[2]{a^2 + 1}}$	Richardson *et al.* (1977)
Weighted Difference Vegetation Index $WDVI = NIR = (aR)$	Richardson *et al.* (1977)
Soil Adjusted Vegetation Index $SAVI = \left(\frac{(NIR - R)}{(NIR + R + L)}\right)(1 + L)$	Huete (1988)
Modified SAVI $MSAVI = \frac{2NIR + 1 - \sqrt{(2NIR + 1)^2 - [8(NIR - R)]}}{2}$	Qi *et al.* (1994)
Transformed SAVI $TSAVI = \frac{[a(NIR - aR - b)]}{(R + aNIR - ab)}$	Baret *et al.* (1989)
Soil Adjusted ratio Vegetation Index $SAVI_2 = \frac{NIR}{[R + (b/a)]}$	Major *et al.* (1990)

ing spatial vegetation patterns and for assessing vegetation dynamics (e.g. Justice *et al.* 1985, Townshend and Justice 1986).

It is well documented that the brightness of soil beneath vegetation influences the interpretation of green vegetation by satellite observations (e.g. Huete *et al.* 1984, 1985, Huete and Jackson 1987, Huete 1988, Qi *et al.* 1994, Qi and Huete 1995). Using ground-based spectral measurements, Huete and Jackson (1987) concluded that light coloured soils produce lower NDVI values than darker soil substrates for equivalent vegetation cover. The problem is particularly noticeable in semi-arid and arid environments where there is less than 30% green canopy cover (Pech *et al.* 1986).

The sensitivity of the NDVI to soil background has generated ample interest in developing other indices. Different research groups have developed alternative VIs for qualitative and quantitative evaluation of vegetation characteristics using spectral measurements (see intensive review in Bannari *et al.* 1995). Richardson and Wiegand (1977) noted that, in scatter plots of red against NIR pixel values, bare soil pixels were aligned along a straight line. This line has been denoted the 'soil line', which can be defined by a linear equation with slope a and intercept b. They modified the four-dimensional 'Tasseled Cap' transformation of Kauth and Thomas (1976) to one with two dimensions for use with the red and NIR bands of Landsat MSS (Multi-Spectral Scanner) data, and developed the Perpendicular Vegetation Index (PVI, table 1). The perpendicular distance of a vegetation pixel to the 'soil line' is a measure of the amount of vegetation. However, Huete *et al.* (1985) found that the PVI is also affected by background soil brightness: brighter soil leads to higher PVI values and vice versa, which is the opposite effect to that on the NDVI. Richardson and Wiegand

(1977) presented also the Weighted Difference Vegetation Index (WDVI, table 1) which is functionally equivalent to the PVI but includes only the slope of the soil line in the equation.

Huete (1988) introduced the Soil Adjusted Vegetation Index (SAVI, table 1) in order to minimize the soil darkness influence. Based on a constant soil adjustment factor, *L*, SAVI minimizes the effect of soil background reflected radiation. Qi *et al.* (1994) developed the Modified Soil Adjusted Vegetation Index (MSAVI, table 1) to further minimize soil background influence by using a variable soil brightness correction factor to replace the constant soil correction factor as used in SAVI.

The Transformed Soil Adjusted Vegetation Index (TSAVI, table 1) is a modification of the SAVI concept that was developed by Baret *et al.* (1989). TSAVI takes into account the soil parameters in the PVI concept and does not apply the correction factor *L* in the SAVI formula. Furthermore, a new version of the SAVI was developed by Major *et al.* (1990); this is referred to as $SAVI_2$ (table 1), which considers whether the soil is either wet or dry, and incorporates the soil line parameter into the calculation.

Different experiments have been conducted by some researchers, using narrow-band field reflectance spectra, to study the influence of different soil backgrounds on VIs (Perry and Lautenschlager 1984, Price 1992, 1993). These experiments took place mostly in agricultural areas with different vegetation covers (Huete *et al.* 1985, Huete and Jackson 1987, Huete 1988, Qi *et al.* 1994, Qi and Huete 1995). They were later extended to satellite-based broadband VIs (Qi and Huete 1995, Huete *et al.* 1997). Liu and Huete (1995) used an analytical approach to examine noise sources in existing VIs, for variable canopy background conditions. Their results showed that among the most intensively used VIs, NDVI had the highest level of noise and error, whereas the soil noise in the SAVI and MSAVI had been partially removed to various degrees.

Elvidge and Chen (1995) compared VIs by means of field reflectance spectra acquired over pinyon pine and sage-bush canopies with different backgrounds. The performance of each vegetation index was evaluated based on its capability to estimate leaf area index (LAI) and per cent green cover. Calculations and comparison of the VIs were based on spectral field data, which were transformed to the broad bands of the satellite sensor. The results of that study showed a background effect for each of the tested VIs.

Rondeaux *et al.* (1996) simulated several VIs for different soil samples and a range of canopy covers. The simulations were performed for a pair of single wavelengths in the red and NIR parts of the spectrum. Analysis showed that indices related to the soil line, such as SAVI, MSAVI and TSAVI, produce better results than the NDVI. The latter gives a very wide range of values with varying background.

The spectral reflectance of soil in the visible spectral bands formed part of numerous studies conducted in the recent past (Escadafal *et al.* 1989, Escadafal 1993, Mulders 1993, Matikalli 1997). Matikalli (1997) investigated the spectral reflectance of different soil samples in the visible and NIR. The research indicated that colour is the main feature used in the identification of soils. For the identification and mapping of soil and geological materials of non-vegetated or sparsely vegetated regions, data acquired by sensors operating in the visible and NIR bands show a useful potential.

As mentioned earlier, soil brightness has a significant impact on VIs (e.g. Qi and Huete 1995, Huete *et al.* 1997). Escadafal and Bacha (1996) developed the Brightness

Index (BI), which applies the reflectance values in two visible bands green (G) and red (R), and the NIR band to calculate the brightness of a surface:

$$BI = (G^2 + R^2 + NIR^2)^{1/2} \quad (1)$$

The fact that the BI includes the NIR part of the spectrum makes this index useful for studying the influence of soil brightness on VIs.

Qi (1993) stated that, in order to evaluate VIs, one should consider four sensitivities of the indices. The author ranked these sensitivities in the following order: vegetation sensitivity, soil background variations, atmospheric conditions, and the sensor viewing geometry. The current study deals only with the second priority in vegetation index evaluations—soil background variations (soil brightness). This issue is especially important for global change studies and arid and semi-arid applications where the vegetation is sparse and, therefore, the soil background is the major contributor to the remote sensing signal. For vegetation applications, the primary goal is to minimize the soil noise.

The objective of this paper is to study the sensitivity of different VIs (derived from a Landsat TM image) to bare substrate brightness. It should be emphasized that the evaluation of these VIs for vegetation interpretation in semi-arid environments, with sparse vegetation cover, was beyond the scope of this study. Most of the previous works in this domain deal with correlations between VIs and crop cover, biomass, chlorophyll content and other vegetation parameters, based on spectral field measurements. In this work, only bare surfaces of different brightness and their response to different VIs were studied. Therefore, the correlation between VIs and vegetation parameters such as per cent cover and LAI does not need to be considered. Seven VIs were selected for examination. They belong to two groups; one characterizes the vegetation cover according to the red/NIR slope (NDVI, SAVI and MSAVI) and the other by the perpendicular distance from the bare soil line (PVI, WDVI, $SAVI_2$ and TSAVI).

2. Study area

The Makhtesh Ramon erosive crater (figure 1) is located in the Negev Desert in southern Israel (30°00′–30°15′N and 34°40′–34°50′E). The crater is 40 km long and 7 km wide, covering about 200 km^2 in area. The annual average rainfall is 56 mm, which is restricted to the winter months (October to March). The vegetation cover is less than 15%, consisting mainly of typical desert shrub vegetation, which is located primarily along the riverbeds in the crater (Danin 1983). The annual vegetation varies between years depending on the rainfall amount and distribution.

The erosion crater was formed by the action of the intermittent river Nahal Ramon, which erodes through layers of the Eocene to reveal a variety of substrates otherwise not exposed in this area (Ward *et al.* 1993). The bottom surface of the crater consists of a variety of geological units such as sandstone, gypsum, limestone, dolomite, plutonic crystalline rocks and others (Evenari *et al.* 1982). Table 2 lists the key for the studied lithological/pedological substrates. Figure 1 shows a general geological map of Makhtesh Ramon (Segev 1996). The large variety of geological formations concentrated over such a relatively small area has made it attractive for several remote sensing studies, with the main focus on geology (Kaufmann 1988, Ben-Dor and Kruse 1995, Ben-Dor *et al.* 1996). The Landsat TM image in figure 2 shows the geologic heterogeneity of the surface in Makhtesh Ramon. The boxes show the most interesting parts of the study area with regard to the current study.

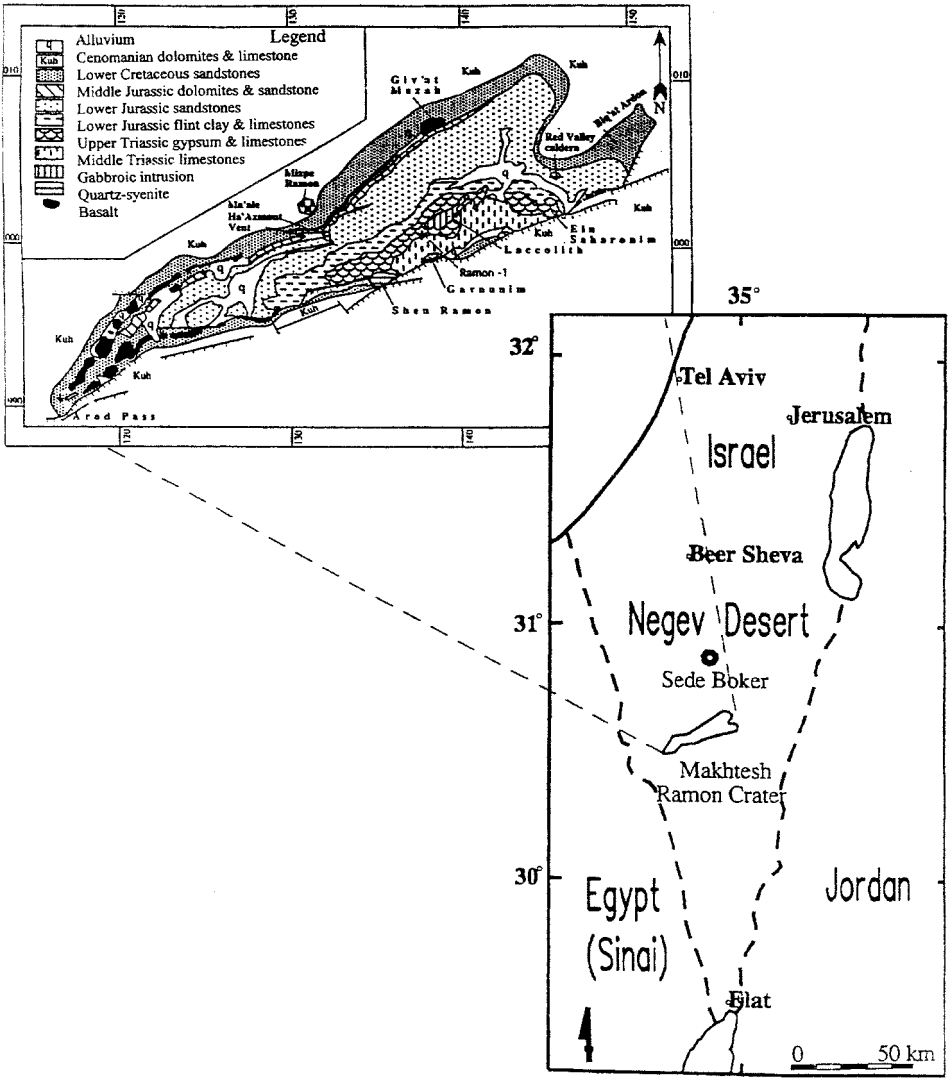

Figure 1. Location map of the study areas and geological map of the Makhtesh Ramon Crater (after Segev 1996).

3. Methodology

3.1. *Satellite data processing*

A Landsat TM image acquired in September 1995 was used for the study. This image, acquired after 6 months of dry weather and high temperatures over the Negev Desert, can be assumed to have detected almost no vegetation signal, only signals of the geological and pedological substrates.

Processing of the Landsat TM image included radiometric, atmospheric and geometric corrections. The radiometric correction procedure was adapted from Markham and Barker (1986). Atmospheric correction of the Top-Of-Atmosphere (TOA) reflectance was carried out using the Second Simulation of the Satellite Signal in the Solar Spectrum algorithm, denoted 6S, version 6 (Vermote *et al.* 1997). For

Table 2. Key for geological substrates with red and NIR reflectances and original VI values based on Landsat TM data.

Key	Geological substrates	Red	NIR	NDVI	SAVI	MSAVI	$SAVI_2$	PVI	WDVI	TSAVI
#1	Basalt	0.100	0.156	0.220	0.089	0.092	1.364	0.002	0.023	0.197
#2	Laccolith	0.116	0.162	0.166	0.072	0.073	1.242	−0.001	0.007	0.138
#3	Sandstone	0.140	0.208	0.197	0.101	0.103	1.346	0.002	0.022	0.182
#4	Sandstone (pediment)	0.166	0.246	0.193	0.112	0.115	1.355	0.003	0.025	0.183
#5	Sandstone (ironoxide)	0.129	0.189	0.189	0.091	0.094	1.319	−0.001	0.017	0.172
#6	Sand (dunes)	0.220	0.326	0.195	0.137	0.140	1.392	0.008	0.033	0.195
#7	Alluvium	0.235	0.346	0.203	0.119	0.122	1.387	0.006	0.029	0.191
#8	Loess/alluvium	0.239	0.350	0.189	0.140	0.143	1.384	0.007	0.031	0.191
#9	Quartzite	0.148	0.222	0.202	0.108	0.111	1.370	0.003	0.025	0.192
#10	Pediment	0.166	0.246	0.201	0.088	0.091	1.319	0.001	0.020	0.191
#11	Limestone (ironoxide)	0.154	0.227	0.190	0.105	0.107	1.342	0.001	0.021	0.179
#12	Limestone (with dolomite)	0.277	0.416	0.200	0.164	0.166	1.426	0.016	0.046	0.206
#13	Kaolinite	0.235	0.327	0.162	0.116	0.118	1.306	−0.004	0.012	0.158
#14	Gypsum	0.220	0.304	0.161	0.110	0.112	1.297	−0.005	0.011	0.155
#15	Flintstone	0.213	0.326	0.211	0.147	0.150	1.435	0.014	0.042	0.212

Figure 2. Subset of Landsat TM image (RGB = 3, 2, 1), acquired in September 1995, showing the Makhtesh Ramon Crater. The red boxes mark the areas with the most significant differences between the vegetation indices.

this program the desert model was selected. Measurements of the aerosol optical thickness and the precipitable water were obtained by an automatic Sun tracking photometer (CIMEL) (Holben *et al.* 1998). This instrument is located at the site of the Jacob Blaustein Institute for Desert Research, Ben-Gurion University of the Negev, Sede Boker Campus, about 30 km north of the study area. Values for ozone concentration were determined from climatological data, based on the Total Ozone Mapping Spectrometer measurements (TOMS 1993) taken onboard the Nimbus-7 spacecraft between 1987 and 1993.

The image was rectified using well distributed control points. A first-order polynomial equation of the ERDAS Imagine image processing package was used to convert the file coordinates to rectified map coordinates in the Israeli Grid coordinate system (ERDAS 1994).

3.2. *Satellite data analysis*

Seven different VIs were determined (table 1). To calculate the soil line, the lower values of the red versus NIR reflectance scatter plots were used. A simple linear regression between them was used to calculate the slope a and intercept b values of the soil line (figure 3). For SAVI the soil adjustment factor L was used in addition. As suggested by Huete (1988), $L = 1$ was selected due to the sparse vegetation conditions of the study area.

Based on the calculation of the seven VIs, homogeneous substrates, characterized by low standard deviation of VI ranges, were identified. Each substrate represents a different lithology or pedology. Since the dynamic ranges of the VIs are different

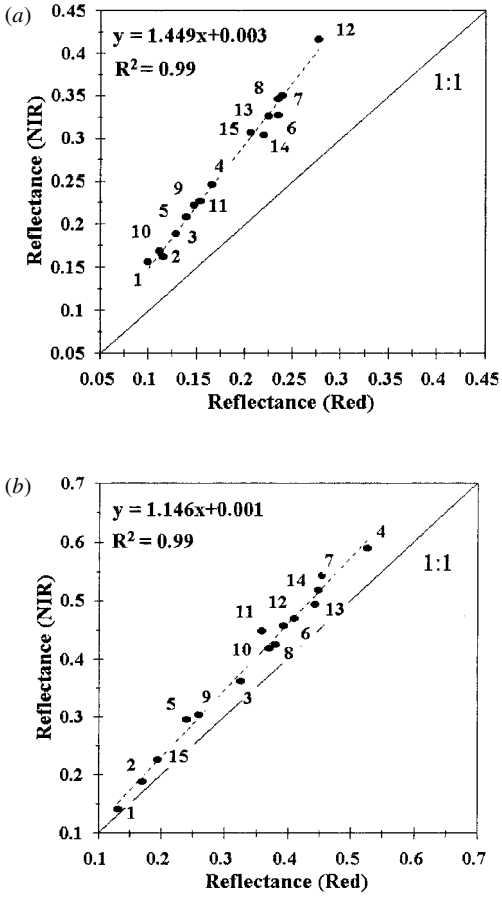

Figure 3. Scatter plots of NIR against red reflectances of the bare surface materials (for key to numbers see table 2) in the study area, showing tendency towards the NIR as the reflectance values increase: (*a*) Landsat TM data and (*b*) laboratory spectral measurements.

from one another, and a few of them can have negative values, it is impossible to compare them directly. Therefore, qualitative comparison between the VIs was performed after rescaling them to values in the range of 0 to 1, based on the following formula:

$$VI_{rescaled} = (VI_{value} - VI)/(VI_{max} - VI_{min}) \quad (2)$$

where, for a given VI type, the subscripts value, min, max and rescaled designate the original, minimum, maximum and rescaled values respectively. Besides the VIs, the Brightness Index (BI) was calculated for each substrate type, using equation (1), based on the method of Escadafal and Bacha (1996). This was in order to study the relationship between the VI and the BI values of the different bare surface types.

3.3. *Laboratory measurements*

Substrate samples were collected from different locations in the Makhtesh Ramon Crater. Samples varied from black basalt (#1) to very bright gypsum (#14). For each

sample, reflectance values were measured in the laboratory at wavelengths of between 400 and 1100 nm using a LICOR spectrometer (LI-COR 1989). A 1000 W halogen lamp was used as a light source. Reflected radiation was measured with a 15° field-of-view from a height of 50 cm above the samples. An average value of four reflectance measurements for each sample was calculated, each obtained after rotating the sample 90° in the horizontal plane. The VI and BI values were calculated to correspond with the spectral bandwidth of the Landsat TM sensor.

4. Results and discussion

It is assumed that the reflectance values acquired by the Landsat TM were entirely from the substrate rather than vegetation since, in addition to the low vegetation cover, most of the plants were almost completely dry at that time of the year. Figure 3 shows the soil base lines resulting from interpolations between the low values from the red and NIR scatter plots of all substrates. The difference between red and NIR becomes larger as the brightness of the substrate increases. Therefore, the distance from the 1:1 line increases with substrate brightness. The slope of the soil base line reflects the sensitivity of the VI to the bare surface materials. Higher slope values may cause higher VI values. Figure 3(*a*) shows the soil base line for the Landsat TM data. In comparison with figure 3(*b*), which represents the laboratory spectral measurements, the slope of the soil base line in figure 3(*a*) is steeper and shifts significantly from the 1:1 line with increasing surface brightness. This phenomenon is slightly less pronounced for the laboratory spectral measurements (figure 3(*b*)). The high slope in the soil line, measured by the Landsat TM sensor in the red and NIR, might be caused by sparse cover of dead plant material in some of the study areas (limestone #12). Table 2 lists the reflectances in red and NIR as well as the original VI values for each substrate. All the parameters show a wide range of values for the bare surfaces. The relative difference between red and NIR increases with brightness of substrate, as can be seen in figure 3(*a*).

The correlation matrix between pairs of the seven VIs based on Landsat TM data is shown in table 3. Very high correlation coefficients were found between SAVI and MSAVI ($r^2 = 0.999$), WDVI and PVI ($r^2 = 0.997$), $SAVI_2$ and WDVI ($r^2 = 0.930$), $SAVI_2$ and PVI ($r^2 = 0.919$), and $SAVI_2$ and TSAVI ($r^2 = 0.951$). The lower coefficients of the other pairs are mainly due to the extreme dark or bright substrates such as basalt (#1), laccolith (#2), kaolinite (#13) and flintstone (#15). This can be noticed from the high residual values of the different substrates in the regression plots (figures 4(*a*)–(*f*)). For example, in figure 4(*a*), basalt (#1) is represented by a high

Table 3. Correlation coefficients (r^2) between pairs of vegetation indices of bare surface materials derived from the Landsat TM image of the Makhtesh Ramon Crater. Bold numbers indicate relatively high correlation.

	NDVI	SAVI	MSAVI	$SAVI_2$	TSAVI	PVI	WDVI
NDVI	*1.000*						
SAVI	0.030	*1.000*					
MSAVI	0.036	**0.999**	*1.000*				
$SAVI_2$	0.473	0.681	0.695	*1,000*			
TSAVI	0.659	0.484	0.499	**0.951**	*1,000*		
PVI	0.407	0.713	0.721	**0.919**	**0.843**	*1.000*	
WDVI	0.404	0.723	0.732	**0.930**	**0.857**	**0.997**	*1.000*

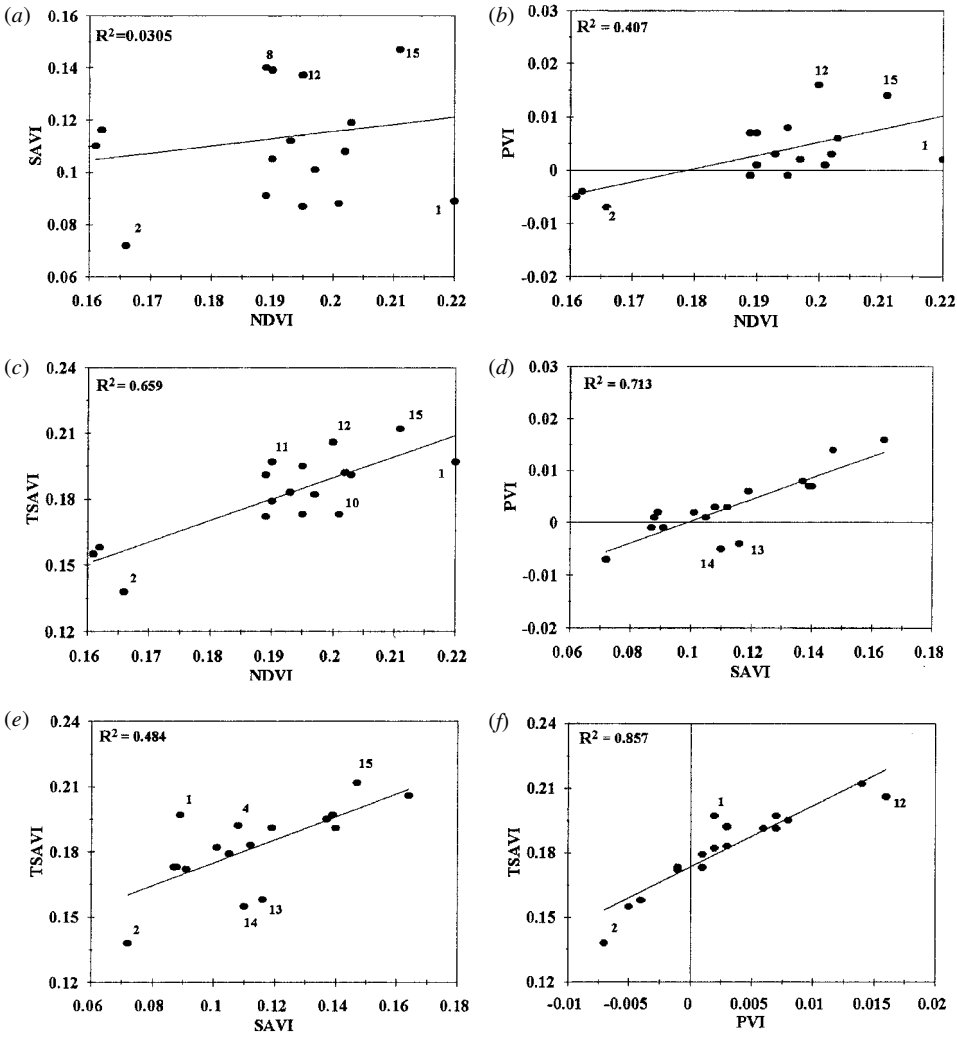

Figure 4. Correlation between pairs of the selected vegetation indices based on Landsat TM analysis.

NDVI value but low SAVI value, thereby having a high residual value. A similar effect can be noticed for bright surface materials. For example, the SAVI value of loess (#8) is much higher in relation to the NDVI value of the same material (figure 4(*a*)). Based on these results, the number of VIs used for further study in this paper was reduced to four—the indices which showed least correlation in their sensitivity to the substrate (NDVI, SAVI, PVI and TSAVI). Analysis of the laboratory spectral measurements showed very similar high correlations for SAVI versus MSAVI, for PVI versus WDVI and TSAVI versus $SAVI_2$.

Table 4 lists the rescaled VI values that were extracted from the Landsat TM image for the selected substrates. The italicized entries represent substrates with high variation between rescaled VIs. The BI values of the substrates based on the spectral laboratory measurements are also listed. The strong sensitivity of NDVI for dark substrates is underlined by the high NDVI for basalt (#1), which is more than double

Table 4. Rescaled vegetation index values based on Landsat TM analysis and brightness index values based on spectral laboratory measurements. Italic numbers indicate substrates with significant variation between the VIs.

Key	Lithological/pedological substrates	NDVI	SAVI	PVI	TSAVI	Brightness index
#1	Basalt	*0.699*	*0.282*	*0.400*	*0.564*	*0.221*
#2	Laccolith	0.175	0.153	0.175	0.288	0.283
#3	Sandstone	0.476	0.374	0.400	0.493	0.540
#4	Sandstone (pediment)	0.437	0.458	0.425	0.498	0.895
#5	Sandstone (ironoxide)	0.398	0.404	0.375	0.479	0.453
#6	Sand dunes	*0.456*	*0.649*	*0.550*	*0.553*	*0.662*
#7	Alluvium	*0.408*	*0.664*	*0.525*	*0.535*	*0.315*
#8	Loess/alluvium	*0.398*	*0.672*	*0.525*	*0.535*	*0.645*
#9	Quartzite	0.524	0.427	0.425	0.539	0.444
#10	Pediment	*0.514*	*0.275*	*0.375*	*0.451*	*0.638*
#11	Limestone (ironoxide)	0.408	0.404	0.375	0.479	0.622
#12	Limestone (with dolomite)	*0.505*	*0.855*	*0.755*	*0.605*	*0.698*
#13	Kaolinite	*0.136*	*0.488*	*0.255*	*0.381*	*0.771*
#14	Gypsum	*0.126*	*0.443*	*0.225*	*0.367*	*0.774*
#15	Flintstone	0.612	0.725	0.700	0.632	0.333

the SAVI for the same substrate. The opposite is observed for bright substrates such as loess (#8), limestone (#12), kaolinite (#13) and gypsum (#14), for which the NDVI is lower than all the other VIs. For some materials (e.g. sandstone and sanddune (#3, 4, 5, 6)) all four VIs respond quantitatively similarly. The laccolith (#2) is characterized by small values for all VIs, whereas flintstone (#15) shows a high response in all Landsat TM based VIs.

Figure 5 shows images of four of the rescaled VIs for the central part of the Makhtesh Ramon Crater. In this area gypsum (#14) and laccolith (#2) are the main lithological/pedological substrates. As seen in figure 5(*a*), the gypsum (indicated by an arrow) is represented by low NDVI values, while SAVI (figure 5(*b*)) shows relatively higher rescaled VI values for the same area. These results emphasize the observed phenomenon of low response of NDVI to bright surface types. This is in contrast to SAVI, which represents these bright materials with much higher values. PVI shows a similar response to NDVI, while TSAVI is close to SAVI. Figure 6 illustrates the same VIs, but for a different zone located in the western part of the study area. As can be seen in the Landsat TM image (figure 2), this area is covered by distinctive basalt hills. The basalt hills appear in different grey tones on the images of the different VIs (figure 6), which is also obvious from the wide variation in the values representing basalt (#1) in table 4. The NDVI (figure 6(*a*)) values are relatively high, while SAVI (figure 6(*b*)) does not show much sensitivity to the darkness of the substrate. PVI (figure 6(*c*)) appears to show almost the same response as SAVI, while TSAVI (figure 6(*d*)) shows slightly higher values for the basalt than SAVI or PVI.

The previous comparison of all VIs shows that NDVI, SAVI, PVI and TSAVI respond differently to variability in bare surface material. Correlation analysis between the brightness values from the laboratory spectral measurements and those of the Landsat TM analysis, for the main substrates, gave a high value of $r^2 = 0.79$. To summarize the relationship between brightness and VIs quantitatively, the BI and VI values based on the Landsat TM data were correlated (table 5). High

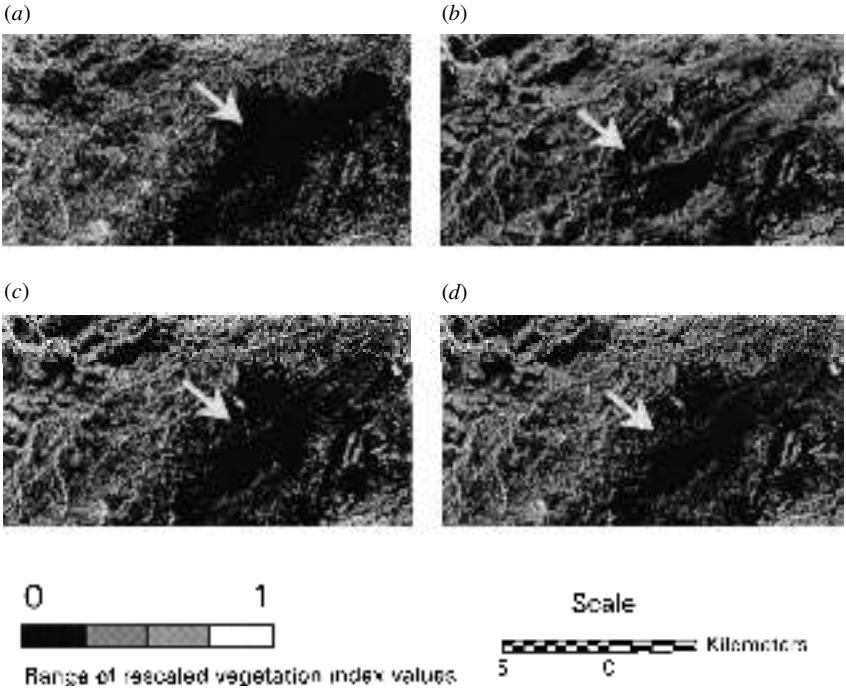

Figure 5. Greyscale images of the rescaled vegetation indices for the central part of the Makhtesh Ramon Crater. White arrows show the location of the gypsum area. The rescaled vegetation index values range from 0 (black) to 1 (white). (*a*) NDVI, (*b*) SAVI, (*c*) PVI, (*d*) TSAVI.

correlation between the BI and any VI means that the VI of the bare surface is very sensitive to the brightness of the substrate material. As seen in table 5, NDVI does not show any correlation, SAVI shows a strong correlation, whereas PVI and TSAVI show very little correlation with the surface brightness in the Landsat TM data. Since the sensitivity of satellite-derived VIs to surface brightness is a chief interest of this work, it is worthwhile examining the regression plots (figure 7) between the Landsat TM derived VI and BI values of the selected bare surfaces. The NDVI shows a weak correlation with soil brightness, with only a slight decrease as a function of brightness (figure 7(*a*)). The high NDVI value for basalt (#1) has contributed immensely to this result. SAVI shows high positive correlation with the BI of the surface material (figure 7(*b*)). PVI (figure 7(*c*)) and TSAVI (figure 7(*d*)) also increase with increasing BI, but with a reduced correlation compared to SAVI.

The difference between the rescaled VIs was calculated in order to detect the sensitivity and different responses of the VIs to the brightness of various substrates. Figure 8 shows the difference between the rescaled NDVI and SAVI for the entire study area. The white and black areas are locations of extreme difference in response between the two VIs. White areas represent high NDVI values, while black areas show high SAVI values. Figure 9 shows the relationship between surface brightness and various VI pair differences. The difference between SAVI and NDVI ($\Delta_{\mathrm{SAVI-NDVI}}$) correlated highly positively ($r^2 = 0.89$) with substrate brightness (figure 9(*a*)). The high correlation shows that the difference in the responses of SAVI and NDVI for

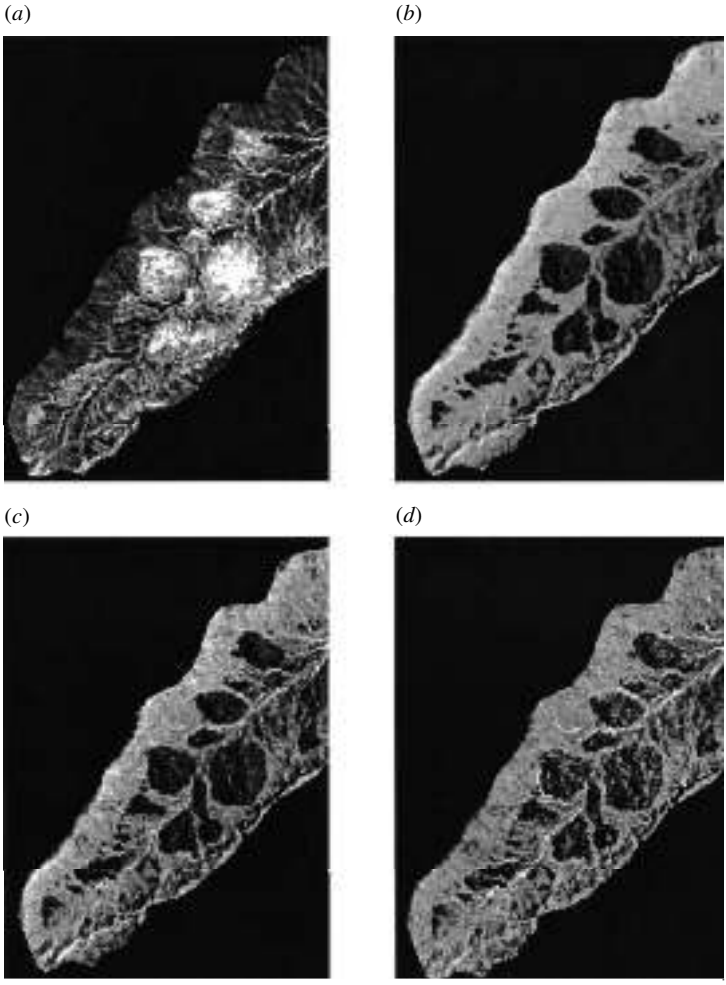

Figure 6. Greyscale images of the rescaled vegetation indices for the western part of the Makhtesh Ramon Crater focused on the basalt hills. The rescaled vegetation index values range from 0 (black) to 1 (white). (*a*) NDVI, (*b*) SAVI, (*c*) PVI, (*d*) TSAVI.

Table 5. Correlation coefficients (r^2) between brightness values and vegetation index values based on Landsat TM data of bare surface material in the Makhtesh Ramon Crater.

	Landsat TM data
NDVI	0.055
SAVI	**0.835**
TSAVI	0.125
PVI	0.323

the same bare surface material depends on the brightness of the substrate. As shown in figure 9(*a*) and figure 8, NDVI responds to dark surface material with much higher values than SAVI (positive Δ_{VI}). The same behaviour has been found for $\Delta_{PVI-NDVI}$ (figure 9(*b*)), $\Delta_{TSAVI-NDVI}$ (figure 9(*c*)) and $\Delta_{SAVI-PVI}$ (figure 9(*d*)). These three Δ_{VI}

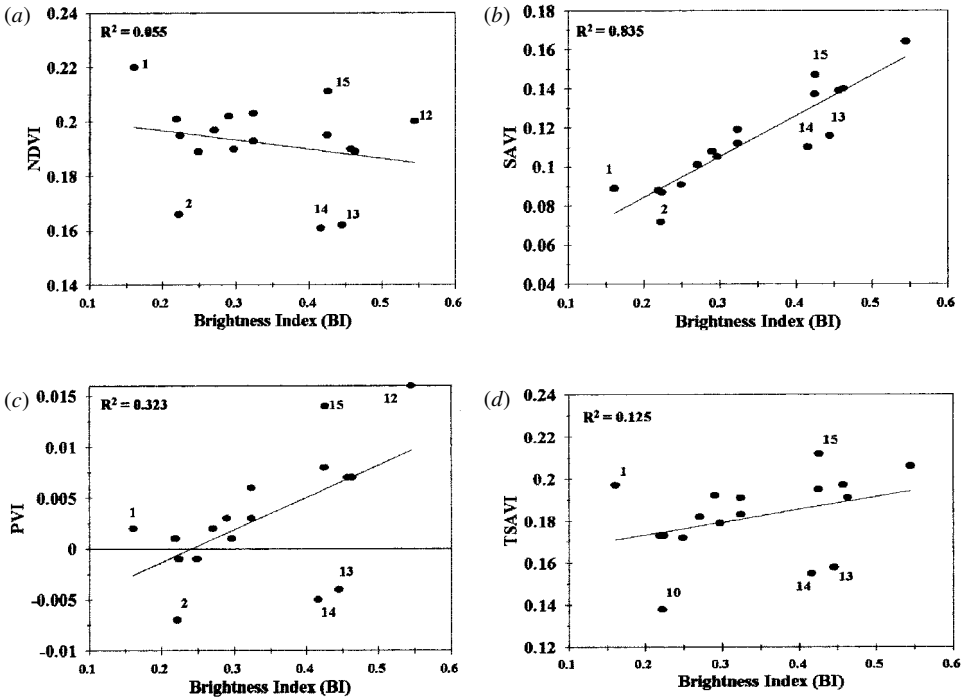

Figure 7. Correlation between vegetation index values and brightness index values of selected bare surface materials; based on Landsat TM data: (*a*) NDVI, (*b*) SAVI, (*c*) PVI and (*d*) TSAVI.

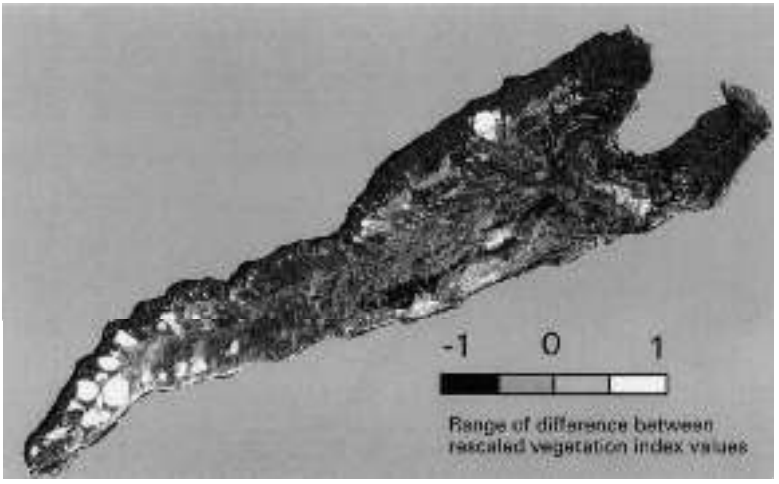

Figure 8. Difference image ($\Delta_{NDVI-SAVI}$) of the Makhtesh Ramon Crater.

increase as a function of the substrate brightness, except that the slopes of their regression lines are different. The slope for $\Delta_{SAVI-NDVI}$ (1.917) is much higher than for $\Delta_{PVI-NDVI}$ (1.106), $\Delta_{TSAVI-NDVI}$ (0.595) and $\Delta_{SAVI-PVI}$ (0.81). Therefore, the dependence of $\Delta_{SAVI-NDVI}$ on surface brightness exceeds those of $\Delta_{PVI-NDVI}$, $\Delta_{TSAVI-NDVI}$ and $\Delta_{SAVI-PVI}$. As can be seen in figures 9(*b*) and 9(*c*), the different responses of basalt

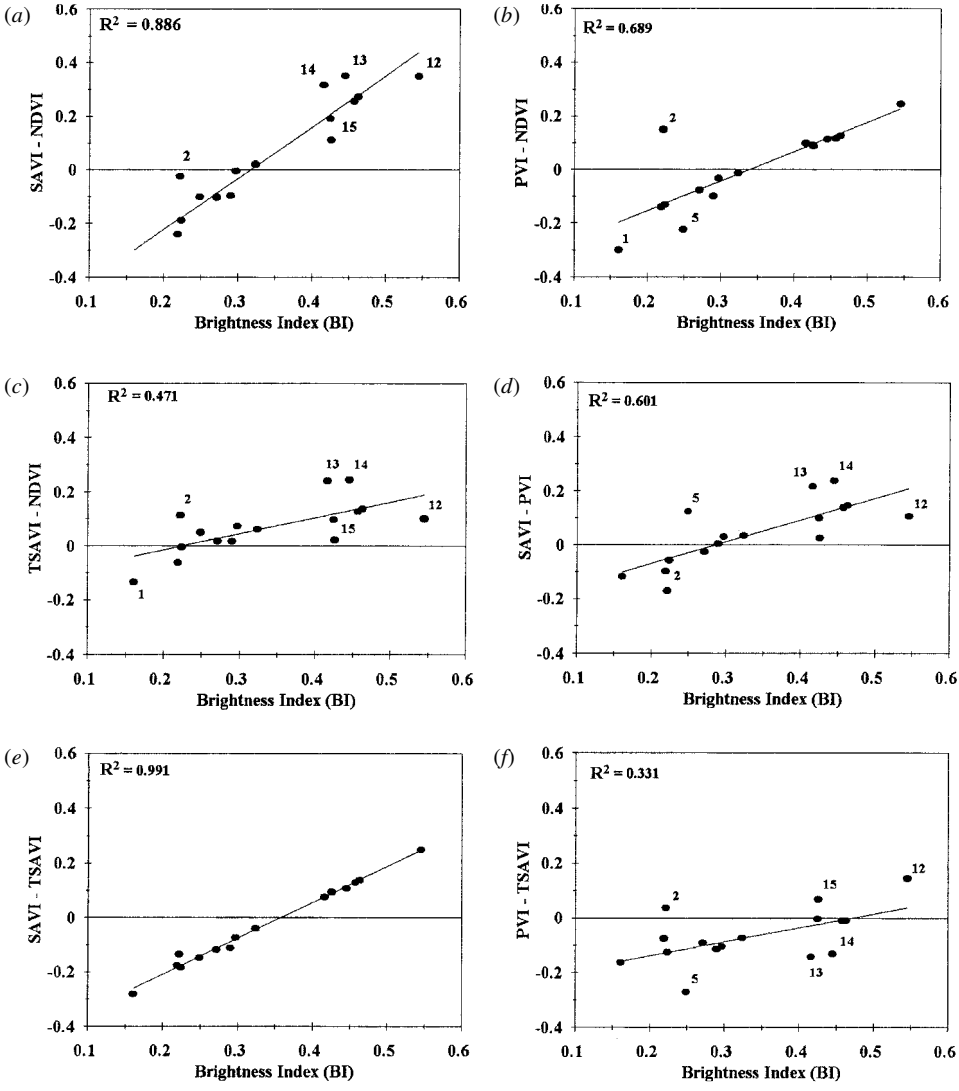

Figure 9. Correlation between brightness and rescaled VI differences (Δ_{VI}) for selected bare surface materials, based on Landsat TM data.

(#1) and laccolith (#2) in these VIs does not have strong dependence on the brightness of both surface components. $\Delta_{SAVI-TSAVI}$ in figure 9(*e*) shows the highest correlation with substrate brightness ($r^2 = 0.991$). This is probably because, in general, TSAVI shows much higher values for dark surface types, while SAVI responds more sensitively to brighter surface materials. Furthermore, the slope of the regression line is relative high (0.462). The difference between PVI and TSAVI ($\Delta_{PVI-TSAVI}$) shows a weak correlation as a function of substrate brightness ($r^2 = 0.331$) (figure 9(*f*)).

5. Conclusions

Soil background is a major surface component that has an impact on the spectral behaviour of vegetation canopies, especially in semi-arid environments with sparse

vegetation cover. The goal of this paper has been to show that the values of the VIs vary not only as a function of the vegetation, but also due to variation in the exposed soil or rock background in terms of the substrate brightness. Therefore, the results presented here are specific to the sensitivity of VIs to bare surface material rather than to vegetation. The sensitivity of different VIs to bare surface materials and their Landsat TM derived brightness was investigated and the effect of different background substrates on the most widely used VIs was examined.

Out of the seven VIs investigated, it was found that three different pairs have such a high correlation that one member of each pair can be practically considered the same index as the other. In effect, SAVI and MSAVI show almost the same sensitivity to bare surface materials. The same phenomenon was observed also for PVI and WDVI, and for $SAVI_2$ and TSAVI. The main indices that show considerable variation between them are NDVI, SAVI, PVI and TSAVI.

It was demonstrated that NDVI is very sensitive to basalt and responds with a high value, whereas SAVI and PVI respond to bright surface materials with higher values. Comparison of brightness values with VI values of different bare surface materials underlines the strong dependence of VIs on the brightness variation of the soil background. The high correlation between brightness and Δ_{VI} proves these results. For instance, the difference in response between SAVI and NDVI, and SAVI and TSAVI to bare surface material is caused by brightness variation, while the difference between SAVI and PVI does not show the same strong dependence on brightness.

Acknowledgments

We thank Sveta Gilerman for her essential assistance. We gratefully acknowledge the help of Kevin G. Kleinsah and Iris Schmidt for collecting the substrate samples in the Makhtesh Ramon Crater, and Charles Ichoku for editing the paper. Finally, we also thank the MINERVA-Stipendien-Komitee and the German Academic Exchange Program (DAAD) who financed this work with research fellowships.

References

Bannari, A., Morin, D., Bonn, F., and Huete, A. R., 1995, A review of vegetation indices. *Remote Sensing Reviews*, **13**, 95–120.

Baret, F., Guyot, G., and Major, D. J., 1989, TSAVI: a vegetation index, which minimizes soil brightness effects on LAI and APAR estimation. *Proceedings of the 12th Canadian Symposium on Remote Sensing, IGARRSS'90, Vancouver, BC, Canada, 10–14 July*, volume 3 (Piscataway, NJ: IEEE), pp. 1355–1358.

Ben-Dor, E., and Kruse, F. A., 1995, Surface mineral mapping of Makhtesh Ramon Negev, Israel using GER 63 channel scanner data. *International Journal of Remote Sensing*, **16**, 3529–3553.

Ben-Dor, E., Kruse, F. A., Dietz, J. B., Braun, A. W., and Banin, A., 1996, Spatial distortion and quantitative geological mapping of Makhtesh Ramon, Negev, Israel, by using the GER 63 channel scanner data. *Canadian Journal of Remote Sensing*, **22**, 258–268.

Danin, A., 1983, *Desert Vegetation of Israel and Sinai* (Jerusalem: Cana).

Elvidge, C. D., and Chen, Z., 1995, Comparison of broad-band and narrow-band red and near-infrared vegetation indices. *Remote Sensing of Environment*, **54**, 38–48.

ERDAS, 1994, Erdas Field Guide, ERDAS Inc., Atlanta, GA, USA.

Escadafal, R., 1993, Remote sensing of soil color: principles and applications. *Remote Sensing Reviews*, **7**, 261–279.

Escadafal, R., and Bacha, S., 1996, Strategy for the dynamic study of desertification. *Proceedings of the ISSS International Symposium Ouagadougou, Burkino Faso, 6–10 February 1995* (Paris: Orstom éditions), pp. 19–34.

Escadafal, R., Girard, M. C., and Courault, D., 1989, Munsell soil color and soil reflectance in the visible spectral bands of Landsat MSS and TM data. *Remote Sensing of Environment*, **27**, 37–46.

Evenari, M., Shanan, L., and Tadmor, N., 1982, The Negev. The Challenge of a Desert (Cambridge: Havard University Press), pp. 437.

Holben, B. N., Eck, T. F., Slutsker, I., Tanré, D., Setzer, A., Vermote, E., Reagan, I. A., Kaufman, Y. J., Nakajama, T., Lavenu, F., Jankowiak, I., and Smirnov, A., 1998, AERONET—A Federated Instrument Network and Data Archive for Aerosol Characterization. *Remote Sensing of Environment*, **66**, 1–16.

Huete, A., 1988, A soil-adjusted vegetation index (SAVI). *Remote Sensing of Environment*, **25**, 295–309.

Huete, A., and Jackson, R. D., 1987, Suitability of spectral indices for evaluating vegetation characteristics on arid rangelands. *Remote Sensing of Environment*, **23**, 213–232.

Huete, A., Jackson, R. D., and Fost, D. F., 1985, Spectral response of a plant canopy with different soil backgrounds. *Remote Sensing of Environment*, **17**, 37–53.

Huete, A., Liu, H. Q., Batchily, K., and van Leeuwen, W., 1997, A comparison of vegetation indices over a global set of TM images for EOS-MODIS. *Remote Sensing of Environment*, **59**, 440–451.

Huete, A., Post, D. F., and Jackson, R. D., 1984, Soil spectral effects on 4-space vegetation discrimination. *Remote Sensing of Environment*, **15**, 155–165.

Justice, C. O., Townshend, J. R. G., Holben, B. N., and Tucker, C. J., 1985, Analysis of the phenology of global vegetation using meteorological satellite data. *International Journal of Remote Sensing*, **6**, 1271–1318.

Kaufmann, H., 1988, Decorrelation processing and evaluation of Landsat TM data as applied to Makhtesh Ramon. *Israel Journal of Earth Sciences*, **37**, 137–143.

Kauth, R. J., and Thomas, G. S., 1976, The tasseled cap—a graphic description of the spatial–temporal development of agricultural crops as seen by Landsat. *Machine Processing of Remotely Sensed Data, Proceedings of LAR Symposium, Purdue University, West Lafayette, Indiana, 29 June–1 July 1976*, edited by P. H. Swain, D. B. Morrison and D. E. Parks (West Lafayette, Ind.: IEEE), pp. 41–51.

LI-COR, 1989, LI-1800 Portable Spectrometer Instruction Manual, Publication No. 8210-0030, LI-COR Inc., Lincoln, NE, USA.

Liu, H. Q., and Huete, A., 1995, A feedback based modification of the NDVI to minimize canopy background and atmospheric noise. *IEEE Transactions on Geoscience and Remote Sensing*, **33**, 457–465.

Major, D. J., Baret, F., and Guyot, G., 1990, A ratio vegetation index adjusted for soil brightness. *International Journal of Remote Sensing*, **11**, 727–740.

Markham, B. L., and Barker, J. L., 1986, Landsat MSS and TM post calibration dynamic ranges, atmospheric reflectance and at-satellite temperature. EOSAT Landsat Technical Notes 1, August 1986, Earth Observation Satellite Company, Lanham, MD, USA, pp. 3–8.

Mattikalli, N. M., 1997, Soil color modeling for the visible and near-infrared bands of Landsat sensors using laboratory spectral measurements. *Remote Sensing of Environment*, **59**, 14–28.

Mulders, M. A., 1993, Remote sensing of soils in warm arid and semi-arid lands. *Remote Sensing Reviews*, **7**, 341–363.

Pech, R. P., Davis, A. W., Lamacraft, R. R., and Graetz, R. D., 1986, Calibration of Landsat data for sparsely vegetated semi-arid rangelands. *International Journal of Remote Sensing*, **7**, 1729–1750.

Perry, C. R., and Lautenschlager, L. F., 1984, Functional equivalence of spectral vegetation indices. *Remote Sensing of Environment*, **14**, 169–182.

Price, J. C., 1992, Estimating vegetation amount from visible and near infrared reflectance measurements. *Remote Sensing of Environment*, **41**, 29–34.

Price, J. C., 1993, Estimating leaf area index from satellite data. *IEEE Transactions on Geoscience and Remote Sensing*, **31**, 727–734.

Qi, J., 1993, Compositing multitemporal remote sensing data sets. Ph. D. dissertation, University of Arizona, Tucson, AZ, USA.

Qi, J., Chehbouni, A., Huete, A., Kerr, Y. H., and Sorooshian, S., 1994, A modified soil adjusted vegetation index. *Remote Sensing of Environment*, **48**, 119–126.

Qi, J., and Huete, A., 1995, A feedback based modification of the NDVI to minimize canopy background and atmospheric noise. *IEEE Transactions on Geoscience and Remote Sensing*, **33**, 457–465.

Richardson, A. J., and Wiegand, C. L., 1977, Distinguishing vegetation from soil background information. *Photogrammetric Engineering and Remote Sensing*, **43**, 1541–1552.

Rondeaux, G., Steven, M., and Baret, F., 1996, Optimization of soil-adjusted vegetation indices. *Remote Sensing of Environment,* **55**, 95–107.

Rouse, J. W., Haas, R. H., Schell, J. A., Deering, D. W., and Harlan, J. C., 1974, Monitoring the Vernal Advancements and Retrogradation (Greenwave Effect) of Nature Vegetation, NASA/GSFC Final Report, NASA, Greenbelt, MD, USA.

Segev, A., 1996, Mesozoic magmatism in the Ramon. *Israel Journal of Earth Sciences*, **45**, 90–100.

TOMS, 1993, Total Ozone Mapping Spectrometer, instrument onboard the Nimbus 7 spacecraft. NASA Goddard Space Flight Center, Laboratory for Atmospheres, Code 916, Greenbelt, MD, USA.

Townshend, J.-R.-G., and Justice, C. O., 1986, Analysis of dynamics of African vegetation using the NDVI. *International Journal of Remote Sensing*, **7**, 1224–1242.

Vermote, E., Tanré, D., Deuze, J. L., Herman, M., and Morcette, J.-J., 1997, Second Simulation of the Satellite Signal in the Solar Spectrum (6S). *IEEE Transactions on Geoscience and Remote Sensing*, **35**, 675–685.

Ward, D., Olsvig-Whittaker, L., and Lawes, M., 1993, Vegetation–environment relationship in a Negev Desert erosion cirque. *Journal of Vegetation Science*, **4**, 83–94.